Journal of Contaminant Hydrology 278 (2026) 104885

Contents lists available at ScienceDirect

Journal of Contaminant Hydrology

journal homepage: www.elsevier.com/locate/jconhyd

Assessing the impacts of afforestation on nitrogen load into the northern gulf of America

Ying Ouyang [a,*], Johnny M. Grace [b], Prem Parajuli [c], Yongshan Wan [d], Yanbo Huang [e]

[a] USDA Forest Service, Southern Research Station, Center for Bottomland Hardwoods Research, 775 Stone Blvd., Thompson Hall, Room 309, Mississippi State, MS 39762, USA
[b] USDA Forest Service, Center for Forest Watershed Research, Southern Research Station, 325 John Knox Rd, STE F-210, Tallahassee, FL 32303, USA
[c] Department of Agricultural and Biological Engineering, Mississippi State University, Mississippi State, MS 39762, USA
[d] Center for Environmental Measurement and Modeling, US EPA, 1 Sabine Island Drive, Gulf Breeze, FL 32561, USA
[e] USDA-ARS Genetics and Sustainable Agriculture Research Unit, Mississippi State University, MS 39762, USA

A R T I C L E I N F O

Keywords:
Afforestation
HAWQS model
Nitrogen load
Northern gulf of America

A B S T R A C T

Eutrophication of the northern Gulf of America (NGOA) (also known as northern Gulf of Mexico) due to excess nutrients has resulted in harmful algal blooms, the development of hypoxic zones, and negative impacts on seafood production, recreational activities, and marine transportation. With a growing recognition of afforestation to maximize timber production and improve water quality, there is a critical need to investigate impacts of afforestation on nitrogen (N) loads to the NGOA. Using the Pearl River Basin (PRB) located in Mississippi and Louisiana along with the HAWQS (Hydrologic and Water Quality System) model and the Kolmogorov-Smirnov (K—S) test, we assessed the impacts of afforestation (by converting all corn and soybean lands in the PRB to mixed-forest lands) on total nitrogen (TN) and nitrate-N loads to the NGOA over a 31-year period from 1990 to 2020. Simulations showed that average annual TN and nitrate-N loads were, respectively, 26% and 28% higher in the base scenario than in the afforestation scenario, with statistically significant differences based on the K—S test. The result indicates that afforestation contributed to a very significant reduction in annual N loading from the PRB to the NGOA, which could occur from enhancing N adsorption and immobilization within forest soils, reducing application of synthetic N fertilizers, and decreasing surface runoff after afforestation. Notably, the magnitude of N load reduction was not directly proportional to the area of cropland conversion, suggesting that other factors, including the specific location of afforestation (e.g., riparian zones), land slope, and the types of tree species planted, may also significantly influence N load. Two distinct daily TN loading phases were observed: 1) a slow-loading phase at daily streamflow $\leq$1200 m^3 s^{-1}, and 2) a fast-loading phase at daily streamflow >1200 m^3 s^{-1}. These findings have not been reported in the literature and underscore the value of strategically designed afforestation for optimizing N load reduction in the Gulf region. Additionally, very few studies have investigated the impacts of afforestation on daily N load to the NGOA, and this study would help fill the research gap.

1. Introduction

The northern Gulf of America (NGOA) (also known as northern Gulf of Mexico) is a key economic region due to its seafood production, recreation, and marine transportation. Eutrophication of the NGO due to excess nutrients such as nitrogen (N) and phosphorus from the Mississippi River Basin (MRB) and other adjacent river basins has resulted in harmful algal blooms and the development of hypoxic zones (Breitburg et al., 2018; Goolsby et al., 2001; Lu et al., 2020; Rabalais and Turner, 2019; Rabalais et al., 2002b; Tian et al., 2020). Goolsby et al. (2001) applied regression models to estimate annual N load from the MRB to the NGOA using historical data. They reported that the average annual total N load into the NGOA was 1,568,000ton $yr^{-1}$from 1980 to 1996, while nitrate-N load increased the most and tripled over a 30-year period between 1970 and 2000. Since then, average annual N loads have remained relatively constant but have shown dramatic interannual variability, largely driven by precipitation. These authors further stated that the major sources of N are from agricultural lands in the Corn Belt

* Corresponding author.
E-mail address: ying.ouyang@usda.gov (Y. Ouyang).

https://doi.org/10.1016/j.jconhyd.2026.104885
Received 25 August 2025; Received in revised form 4 February 2026; Accepted 6 February 2026
Available online 10 February 2026
0169-7722/Published by Elsevier B.V.

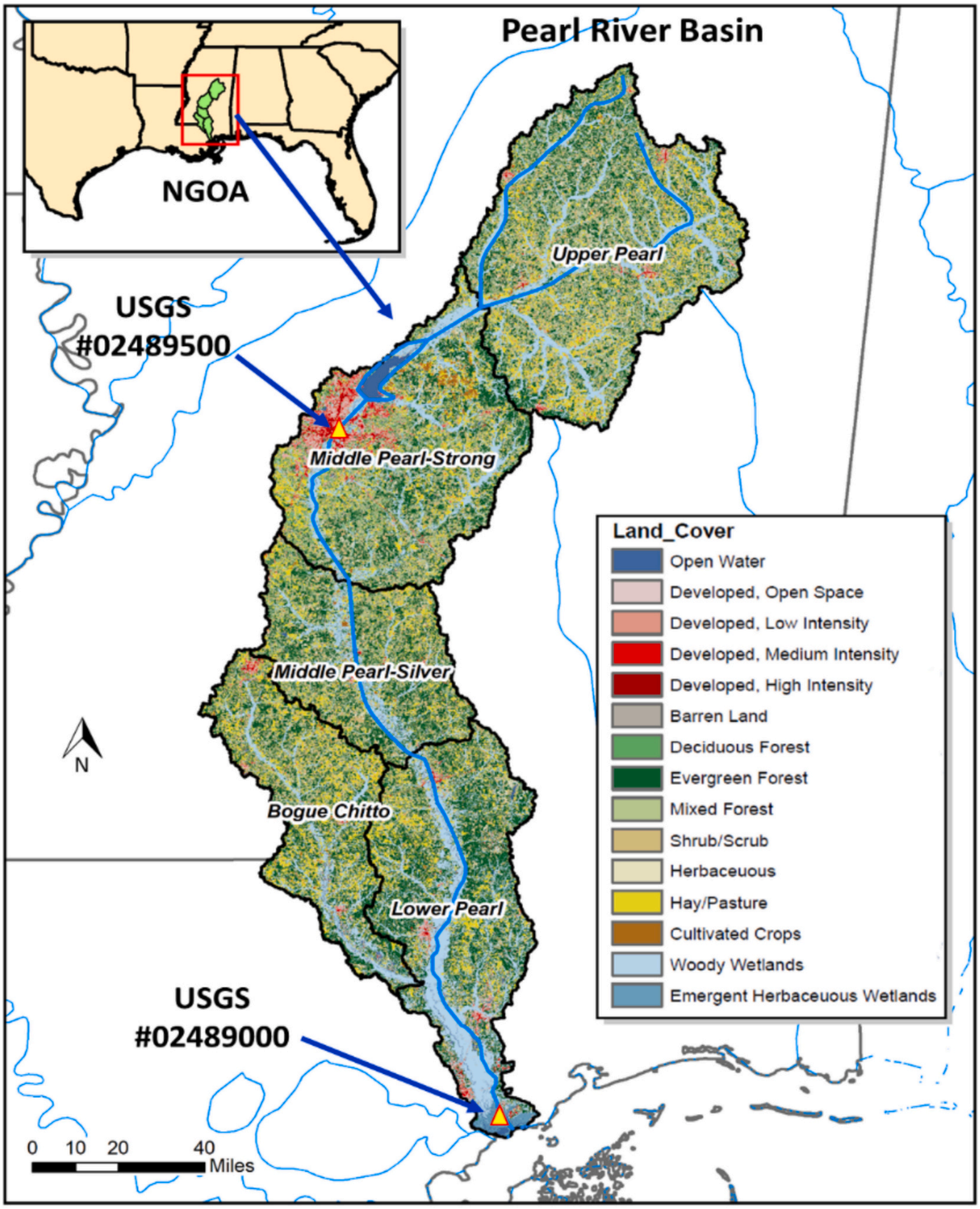

Fig. 1. Location of the Northern Gulf of America, showing the Pearl River Basin and US Geological Survey gauge stations used in this study.

zone, including southern Minnesota, Iowa, Illinois, Indiana, and Ohio. Lu et al. (2020) studied impacts of extreme precipitation on N load from the Atchafalaya River basin, Mississippi to the NGOA using a process-based hydro-ecological model. They found that over 60% of the basin has experienced increased extreme precipitation since 2000, accounting for more than 80% of N leaching loss. Tian et al. (2020) projected the long-term N load from MRB into the NGOA during 1901 to 2014 using the Dynamic Land Ecosystem Model. They reported that total N loads during the first decade of 21st century were twice as high as those in the first decade of the 20th century. These authors further argued that while the N load reduction strategies have been implemented over the past three decades, TN loads into the NGOA have not significantly decreased. These excess N and other nutrients have made the NGOA as one of the world largest human-caused hypoxic zones(with dissolved oxygen $\leq$2 mg L^{-1}), incapable of sustaining normal aquatic life populations (Rabalais et al., 2002b). The seasonal hypoxic zone in the NGOA started in the 1950s and worsen in the 1970s. The bottom area and volume of the hypoxic zone in the NGOA were about 23,000 km^2 and140 km^3, respectively (Rabalais and Turner, 2019). Turner and Rabalais (2022) reported that the size of the hypoxic zone from 1985 to 2019 ranged between 40 and 22,720 km^2 during late July to early August, and averaged 13,829 km^2.

Deforestation refers to the clearing and/or destruction of forests for agriculture, residential and commercial development, and timber harvesting. Deforestation for agricultural expansion in the MRB has resulted in increased loads of nutrients, sediments, herbicides, and pathogens (Dosskey et al., 2012; Goolsby and Battaglin, 2001; Stanturf et al., 2000). Goolsby and Battaglin (2001) reported that N fertilizer application for agriculture in the MRB increased 500% from 1950 to 1970 to 1980–1996, which is the major contributor to a 200% increase in N load

Table 1
Major input parameters and their values used for the base and afforestation simulation scenarios.

Input Variable	Definition/Unit	Base Scenario	Afforestation Scenario
Water Balance			
SFTMP	Snowfall temperature (°C)	−0.8668	−0.8668
SMTMP	Snow melt base temperature (°C)	0.2662	0.2662
SMFMX	Maximum melt rate for snow during the year (occurs on summer solstice) (mm/°C-day)	4.33	4.33
SMFMN	Minimum melt rate for snow during the year (occurs on summer solstice) (mm/°C-day)	3.165	3.165
TIMP	Snow pack temperature lag factor	0.08844	0.08844
IPET	Potential evapotranspiration method (Hargreaves method)	2	2
ESCO	Soil evaporation compensation factor	0.95	0.95
EPCO	Plant uptake compensation factor	1	1
Surface Runoff			
ICN	Daily curve number method	0	1
CNCOEF	Plant ET curve number coefficient	1	1
ICRK	Crack flow code	0	0
SURLAG	Surface runoff lag time	1.079	1.079
OV-N	Manning's “n” value for overland flow	0.14	0.5
CN2 (Corn)	Soil Conservation Service (SCS) runoff curve number for moisture condition II	77–87	65
CN2 (Soybean)	Soil Conservation Service (SCS) runoff curve number for moisture condition II	78–87	65
Nitrogen Cycling			
RCN	Concentration of nitrogen in rainfall (mg N L^{-1})	1	1
CDN	Denitrification exponential rate coefficient	1.5	2
SDNCO	Denitrification threshold water content	0.5	0.5
NPERCO	Nitrogen percolation coefficient	0.5	0.5
Reach			
IRTE	Channel water routing method	0	0
MSK_COL1	Calibration coefficient used to control impact of the storage time constant for normal flow	0	0
MSK_COL2	Calibration coefficient used to control impact of the storage time constant for low flow	3.5	3.5
MSK_X	Weighting factor controlling relative importance of inflow rate and outflow rate in determining water storage in reach segment	0.2	0.2
TRNSRCH	Fraction of transmission losses from main channel that enter deep aquifer	0	0
EVRCH	Reach evaporation adjustment factor	1	1
IDEG	Channel degradation code	0	0
PRF	Peak rate adjustment factor for sediment routing in the main channel	1	1
SPCON	Linear parameter for calculating the maximum amount of sediment that can be reentrained during channel sediment routing	0	1
SPEXP	Exponent parameter for calculating sediment reentrained in channel sediment routing	1	1
IWQ	In-stream water quality code	1	1
ADJ_PKR	Peak rate adjustment factor for sediment routing in the subbasin (tributary channels)	0.5	0.5

from the MRB to the NGOA. Despite numerous studies investigating the ecological and environmental impacts of deforestation in the NGOA (Chakravarty et al., 2021; Rabalais et al., 2002a; Rabalais et al., 2007), few efforts have assessed the potential reduction of afforestation and forest restoration on N load in the coastal watersheds adjacent to the NGOA. Afforestation is the establishment of a forest or stand in an area where the preceding vegetation or land use is not a forest. It can help mitigate surface water runoff, filter pollutants, and reduce nutrient and sediment loads entering surface water bodies (Haghverdi and Kooch, 2020; Mitsch and Day, 2006; Ouyang et al., 2015; Qiu et al., 2022).

With growing recognition of the role of afforestation in supporting timber production, improving water quality, and sustaining terrestrial and aquatic life, including seafood production and recreation, there is a critical need to investigate its impact on N load into the NGOA. The aim of this study was to estimate the impacts of afforestation on N loading into the NGOA using the HAWQS (Hydrologic and Water Quality System) model. The Pearl River Basin (PRB), located in Mississippi and Louisiana, was selected as the study site (Fig. 1). Our specific objectives were to: 1) develop site-specific HAWQS models for simulating N loads from the PRB into the NGOA, including model calibration and validation; 2) compare simulated N loads between afforested and non-afforested land scenarios using the Kolmogorov-Smirnov (K—S) test; and 3) identify key factors contributing to N load reductions following afforestation.

2. Materials and methods

2.1. Study site

The PRB has a drainage area of 22,533 km^2 and encompasses 24 counties in Mississippi and three parishes in Louisiana(MDEQ, 2007). The Pearl River originates in east-central Mississippi and flows into the NGOA. The PRB consists of five watersheds, the upper Pearl River (6379 km^2), middle Pearl-Strong River (5120 km^2), middle Pear-Silver River (3156 km^2), Bogue Chitto River (3130 km^2), and Lower Pear River (4717 km^2) watersheds(Ouyang et al., 2023). Average annual precipitation is 1412 mm, with a wet season from November to April and a dry season from May to October. Average maximum temperature is 33.4 °C in summer and average minimum temperature is 0.3 °C in winter. The basin is composed of 69% forest, 27% agricultural land, and 3% wetlands and 1% waterbodies (Ouyang et al., 2023), and is dominated by fine sandy loam and silt loam soils (Parajuli, 2010). The PRB contains the largest intact bottomland hardwood forest area (about 14,000 ha) remaining in the southeastern U.S., consisting of mixed hardwood species dominated by various oaks (*Quercus* spp.), sweetgum (*Liquidambar styraciflua*), hickories (*Carya* spp.), and elms (*Ulmus* spp.) (Chapman et al., 2008).

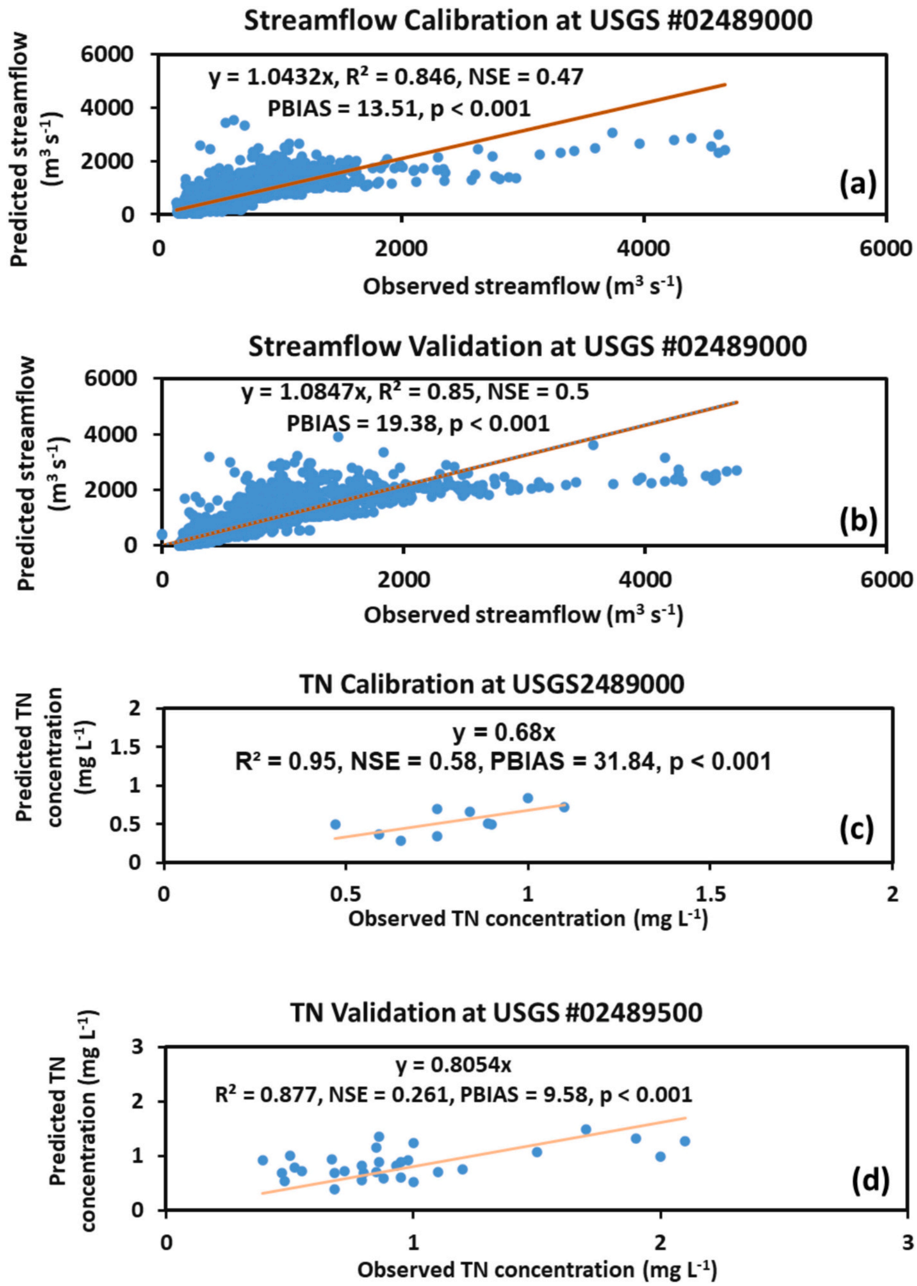

Fig. 2. Comparisons of model predictions and field observations for streamflow and TN concentration during model calibrations and validations.

2.2. HAWQS model development

HAWQS is a customized version of the SWAT (Soil and Water Assessment Tool) model and is a web-based modeling system for simulating water quantity and quality in watersheds across the contiguous United States(HAWQS_2.0, 2023). Advantages of HAWQS include its user-friendly interface with maps; pre-loaded watershed, GIS, and weather data; and post-simulation outputs in tabular, chart, and map formats. Many watershed modeling studies using HAWQS have been reported in the literature(Corona et al., 2020; Fant et al., 2017; Ouyang et al., 2023; Yen et al., 2016). A full description of HAWQS can be found at https://hawqs.tamu.edu/#/. In this study, the HAWQS model for the PRB was developed using the following five major steps:

1. Create a modeling project. Select the watershed that has the basin outlet at a desire Hydrologic Unit Code (HUC) spatial resolution. HAWQS 2.0 provides four resolutions: HUC8 (3691 km^2), HUC10 (518 km^2), HUC12 (98 km^2), and HUC14 (21 km^2). HUC8 was selected because the PRB is a large river basin (Fig. 1).
2. Set up HRUs (Hydrologic Response Units). A1% threshold area of HRUs was used to remove minor land uses, soils and slopes. Land uses occupying <1%of each watershed area in the PRB were omitted to enhance modeling efficiency.
3. Create simulation scenarios. Two simulation scenarios were used. The first (base scenario) simulated N load from the PRB into the NGOA from 1990 to 2019 (31 years) under existing natural conditions and typical agricultural and forest practices. The second (afforestation scenario) was identical, except that all corn and soybean lands in the basin were converted to mixed forest. Comparing the two scenarios provided insights into how afforestation affects N loading into the NGOA. A detailed description of land use conversion is provided in Section 2.3. Table 1 lists major input parameters and their values used in the base and afforestation scenarios.

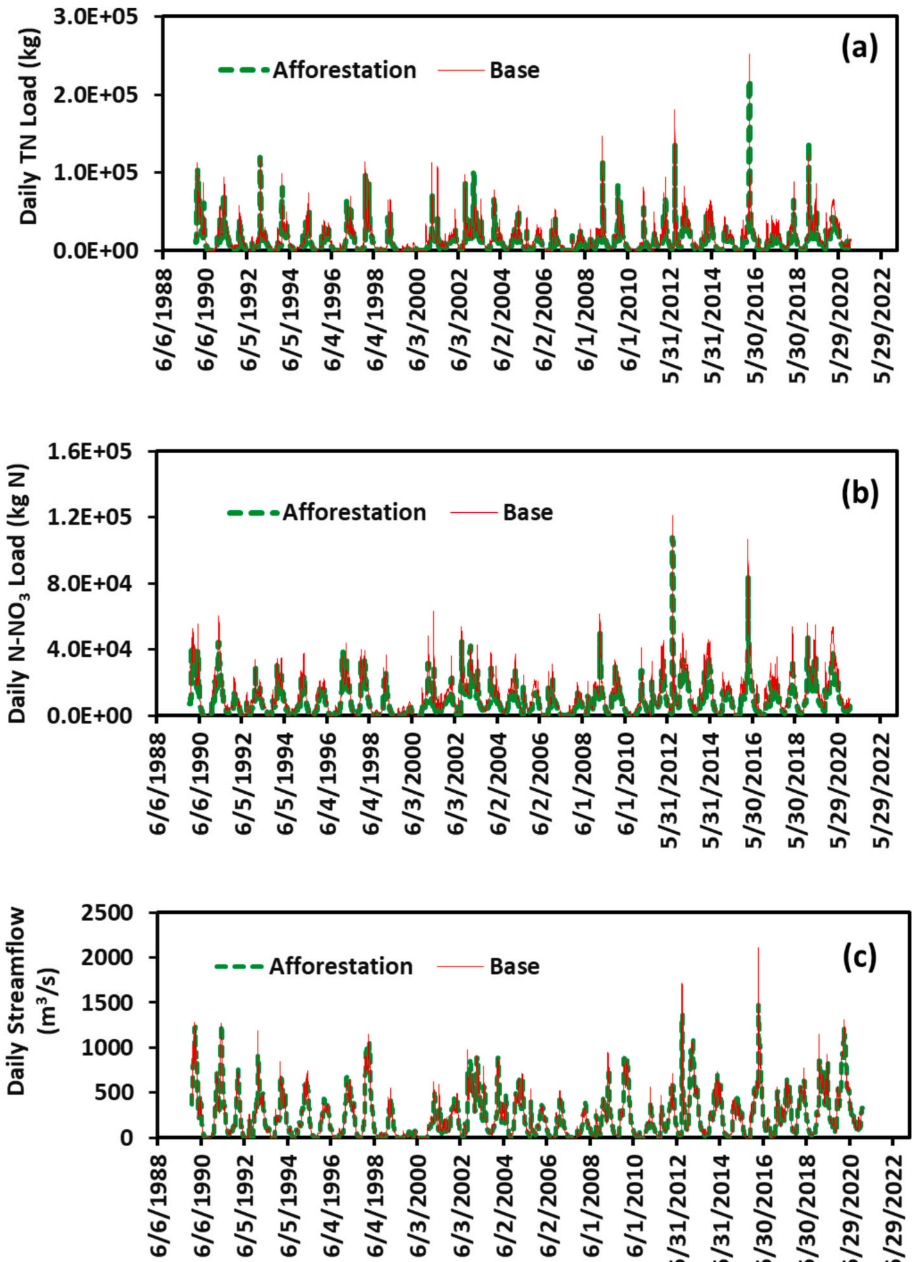

Fig. 3. Daily TN and nitrate-N loads and daily streamflow at the Pear River basin outlet.

4. Customize input data. Major input values listed in Table 1 can be modified in the Customize Input Data section of HAWQS. Historical weather data were obtained from PRISM (Parameter-elevation Regressions on Independent Slopes Model), which is integrated into HAWQS.
5. Run simulations and analyze results. The final step was to run the HAWQS model and evaluate the outputs.

2.3. Input data preparation for land use conversion

HAWQS includes a Land Use Update feature that allows users to modify land uses to assess their impacts on hydrological and water quality processes. Specifically, users can download and edit land use update files to adjust HRU fractions during simulations. In this study, we replaced all of corn (CORN) and soybean (SOYB) land uses (approximately 1% of the total PRB area) in the PRB with mixed forest (FRST) in the land use update file for the afforestation scenario. Accordingly, input parameter values were modified as follows: OV-N = 0.5 (Manning's coefficient for overland flow), CN2 = 65 (Soil Conservation Service runoff curve number for moisture condition II), CDN = 2 (denitrification exponential rate coefficient), and ICN = 1 (improved curve number method), as shown in Table 1. The input parameter values were obtained by referring to the existing FRST land use in the PRB. The land use change was set to begin on 1 January 1985 and end on 31 December 2019, consistent with the base scenario's simulation period. The selection of locations and types of croplands for conversion depends heavily on site-specific conditions and local stakeholder preferences. This study demonstrated a means of evaluating afforestation impacts on N loading into the NGOA. It should be pointed out that while the conversion of the corn and soybean lands to mixed forest lands accounted for only 1% of the entire PRB area. This conversion was equivalent to a 43% reduction of total agricultural land in the PRB.

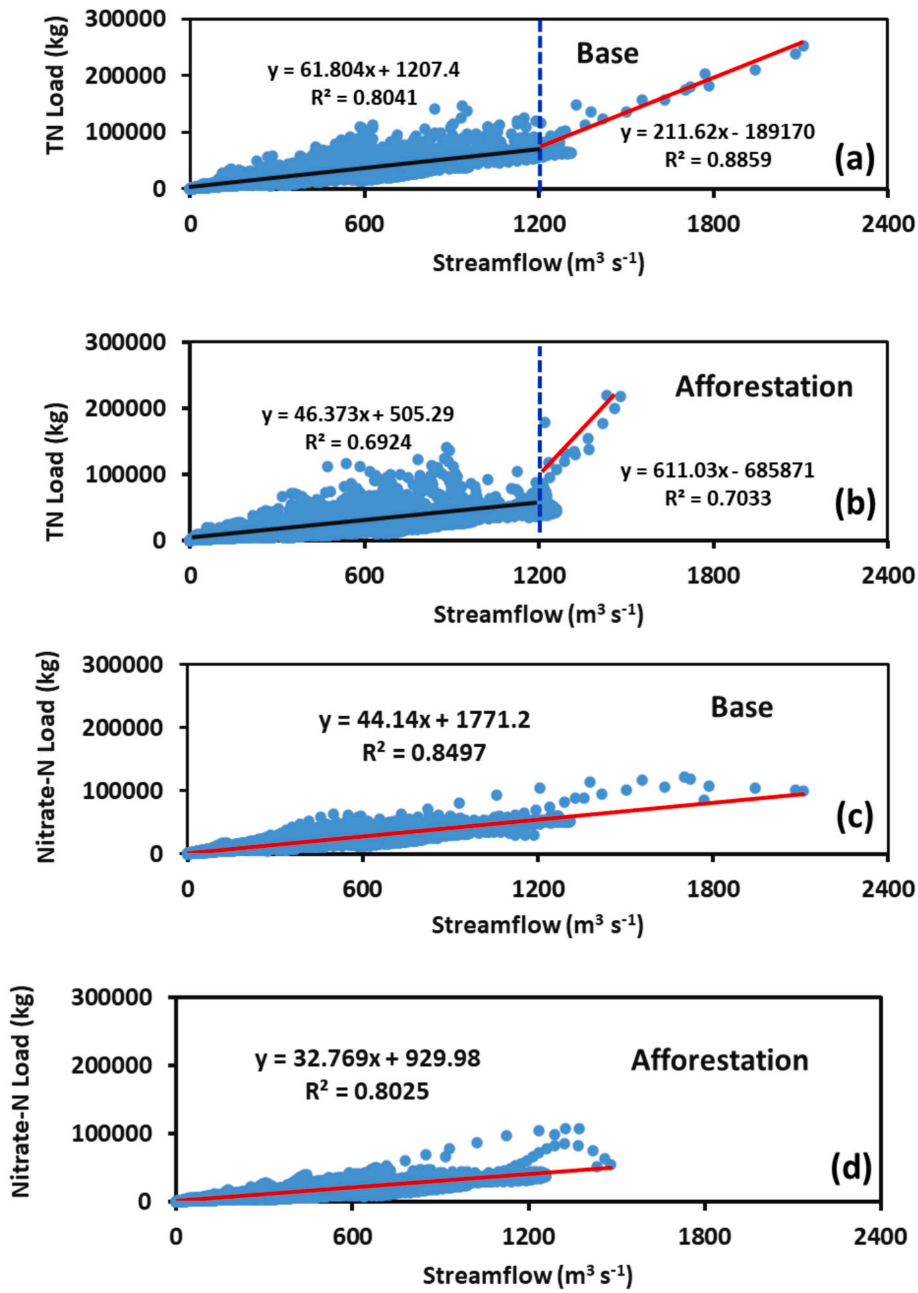

Fig. 4. Daily TN and nitrate-N loads as a function of streamflow for the base and afforestation scenarios.

2.4. Model calibration, validation, and statistics

Model calibration is the process to adjust input parameters values for a close match between model predictions and field observations. In this study, two modeling components were calibrated: hydrology and N. The hydrology component was calibrated with streamflow data, whereas the N component was calibrated with TN concentration data. For the hydrology calibration, observed streamflow data from the USGS gauge station #02489000 (Fig. 1) for the period from 1 January 1999 to 31 December 2008 were used. For the N calibration, observed TN concentration data from the same USGS gauge station for the period from 27 February1974 to 6 June 1975 were selected. It should be noted that observed TN data for the PRB are very limited. The goodness of calibration was evaluated using the Nash-Sutcliffe efficiency (NSE), Percent Bias (PBIAS), Coefficient of Determination (R^2), and *p*-value. Table 1 presents the calibrated parameters and their corresponding values.

Model validation is the procedure of verifying the performance of the calibrated model by comparing predictions against another set of observed data without modifying any input parameter values. For the hydrology validation, streamflow data from USGS station #02489000 for the period 1 January 2009 to 31 December 2018 were used. For the N validation, TN concentration data from USGS station #02489500 (Fig. 1) for the period 6 January 1986 to 14 December 1993 were used. The same statistical metrics used in calibration were applied to assess validation performance.

Differences in streamflow and N loads between the base and afforestation scenarios were assessed using the Kolmogorov - Smirnov (K—S) test. If the D statistic from the K—S test is less than the critical value at $\alpha = 0.05$, the two samples are considered statistically different. In this study, the K—S test was performed using a Python script. The detailed description of the K—S test is described by Solari (1967).

Table 2
Statistical analysis of daily, seasonal, and annual TN and nitrate-N loads and streamflow between the base and afforestation scenarios using the Kolmogorov-Smirnov test. H_o = no difference between the base and afforestation scenarios.

Parameter	Significance Level (α)	D Statistics	Critical Value (n-scaled)	p-value	Result
Daily TN Load	0.05	0.138	0.018	< 0.001	Reject H_o
Daily Nitrate-N Load	0.05	0.144	0.018	< 0.001	Reject H_o
Daily Streamflow	0.05	0.028	0.018	< 0.001	Reject H_o
Seasonal TN Load	0.05	0.202	0.173	0.013	Reject H_o
Seasonal Nitrate-N Load	0.05	0.218	0.173	0.013	Reject H_o
Seasonal Streamflow	0.05	0.048	0.172	0.999	Accept H_o
Annual TN Load	0.05	0.387	0.345	0.018	Reject H_o
Annual Nitrate-N Load	0.05	0.387	0.345	0.018	Reject H_o
Annual Streamflow	0.05	0.065	0.345	1	Accept H_o

3. Results and discussion

3.1. Model performance

Comparisons of model predictions and field observations in daily streamflow during model calibration from 1999 to 2008 as well as during model validation from 2008 to 2017 are shown in Fig. 2. The statistical metrics for R^2, NSE, PBIAS, and *p*-value were, respectively, 0.85, 0.47, 13.51, and < 0.001 for model calibration (Fig. 2a) and were, respectively, 0.85, 0.5, 19.38, and < 0.001for model validation (Fig. 2b). These statistical metrics indicated good model performance in predicting streamflows. Plots of model predictions and field observations in daily TN concentration during model calibration from 1974 to 1975 and during model validation from 1985 to 1993 were also shown in Fig. 2. The statistical values of R^2, NSE, PBIAS, and *p*-value were, respectively, 0.95, 0.58, 31.84, and < 0.001 during model calibration (Fig. 2c) and were, respectively, 0.88, 0.26, 9.58, and < 0.001 during model validation (Fig. 2d). These values demonstrated reasonable model performance in predicting TN concentrations. It should be pointed out here that field observed TN concentrations in the PRB are very limited, which restricts the ability to conduct rigorous model calibration and validation.

3.2. Daily N load

Comparisons of daily TN and nitrate-N loads, along with daily streamflow at the PRB outlet, for the simulation period from 1990 to 2020 (31 years), between the base and afforestation scenarios are shown in Fig. 3. In general, the daily TN load over the 31-year period varied significantly between days in both scenarios (Fig. 3a) and was strongly correlated with variations in daily streamflow (Fig. 3c). In other words, an increase in daily streamflow led to an increase in daily TN load. This occurred because the daily TN load is calculated by multiplying the daily TN concentration by the daily streamflow volume, which is derived by multiplying streamflow rate by the number of seconds in a day. As streamflow rate increases, so does the streamflow volume, and consequently, the TN load.

Two distinct phases of daily TN load were observed in both the base (Fig. 4a) and afforestation (Fig. 4b) scenarios: 1) a slow-loading phase when streamflow was ≤1200 $m^3\ s^{-1}$, and 2) a rapid-loading phase when streamflow exceeded 1200 $m^3\ s^{-1}$. For the base scenario, the slopes of the linear regressions were 61.8 for streamflow ≤1200 $m^3\ s^{-1}$ and 211.62 for streamflow >1200 $m^3\ s^{-1}$ (Fig. 4a), indicating that the slope was approximately 3.4 times steeper above the 1200 $m^3\ s^{-1}$ threshold. A steeper slope implies a more rapid increase in TN load with streamflow. Similar phases were observed in the afforestation scenario (Fig. 4b). These distinct phases of TN load response to streamflow have not been reported in the literature and provide valuable insight for water resource managers, suggesting that reducing streamflow below a critical threshold (1200 $m^3\ s^{-1}$ in this study) could help mitigate daily TN loads. Although the exact reasons for this phenomenon remain to be investigated, a possible explanation would be that as the streamflow increased to a certain rate, the N absorbed in organic matter and sediment located near the bottom of streambeds were mobilized and thus increasing the amount of the N load.

Fig. 3a further shows that daily TN load was higher in the base scenario than in the afforestation scenario. This difference was statistically significant according to the K—S test (Table 2). On average, the daily TN load was 1.6 x 10^4kg in the base scenario and was 1.2 x 10^4kg in the afforestation scenario. The latter was 26% less than the former over the 31-year period. These results demonstrated that the conversion of corn and soybean lands (1% of the total basin area) to mixed forestlands reduced daily TN load from the PRB into the NGOA by about 26%. Very few studies have investigated the impacts of afforestation on daily TN load into the NGOA, and this study helps fill that research gap. Afforestation can immobilize soil N through organic matter adsorption, decrease N levels via plant root uptake, and reduce surface water runoff by intercepting rainfall and acting as a physical barrier to diffuse overland flow. All these processes help mitigate N loading into streams(Li et al., 2014; Rasmussen, 1998; Ryu et al., 2009; Shi et al., 2015).It should also be noted that the specific locations for afforestation play an important role in reducing N load. Afforestation in critical zones such as riparian buffers and riverbanks is more effective at reducing TN loads in streams (Boz and Gumiero, 2016; Jiang et al., 2019; Ouyang et al., 2015).

Jiang et al. (2019) simulated the effects of riparian reforestation on runoff and nutrient reduction in a small watershed in China. They reported that 20 to 60 m widths of riparian buffer reforestation reduced 23 to 56% of TN load into streams. Their findings were within the range of ours.

Changes in daily nitrate-N load over the 31-year period between the base and afforestation scenarios are shown in Fig. 3b. Analogous to the trends observed for TN load, daily nitrate-N loads varied over time and closely followed changes in daily streamflow in both scenarios (Fig. 4c and d). That is, an increase in daily streamflow led to an increase in nitrate-N load, for the same reasons explained earlier regarding TN loads. Differences in daily nitrate-N loads between the base and afforestation scenarios were also statistically significant based on the K—S test (Table 2). The average daily nitrate-N load was 1.2 x 10^4kg in the base scenario and 8.7 x 10^3kg in the afforestation scenario. The latter was approximately 28% lower than the former over the 31-year period, indicating that afforestation reduced the daily nitrate-N load. In general, TN includes organic N, ammonia-N, nitrite-N, and nitrate-N. Based on this study, the daily nitrate-N load accounted for about 30% of the daily TN load in the base scenario and 33% of the daily TN load in the afforestation scenario. These findings contrast with results reported by Goolsby et al. (2001),who used historical data and regression models to show that the annual load of nitrate-N was higher than those of other nitrogen species from the MRB into the NGOA (approximately 61% nitrate as N, 37% organic N, and 2% ammonium as N). Ouyang et al. (2015) estimated effects of afforestation on nitrate-N load reduction in the lower Yazoo River watershed, Mississippi. They reported that an increase in forest lands reduced nitrate-N load because forest soils enriched in organic matter absorb nitrate-N, reduce soil erosion, and decrease surface runoff.

Unlike the case of daily TN load, no distinct phase of daily nitrate-N

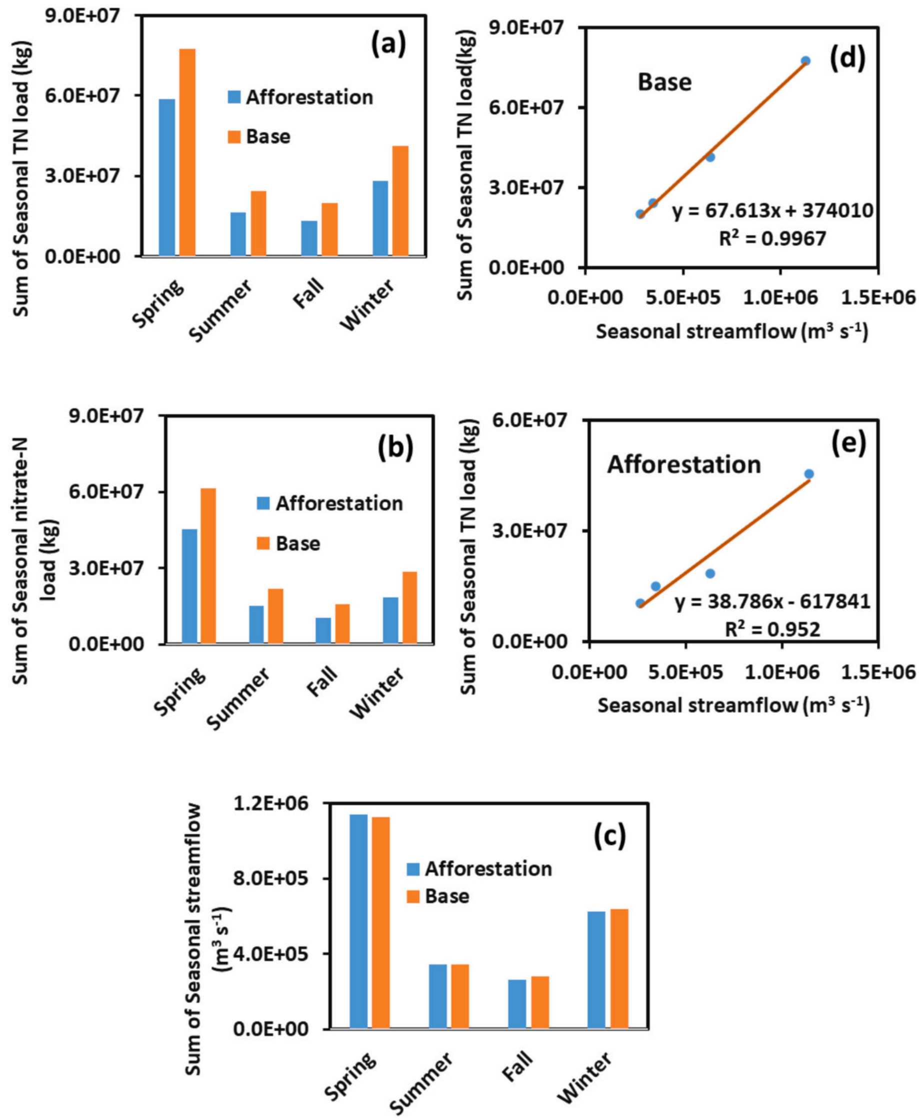

Fig. 5. Seasonal TN (a) and nitrate-N (b) loads and seasonal streamflow (c) as well as seasonal TN (d) and nitrate-N (e) loads as a function of seasonal streamflow in the base and afforestation scenarios.

load as a function of streamflow were observed in either the base (Fig. 4c) or afforestation (Fig. 4d) scenarios. In other words, a single linear relationship adequately described daily nitrate-N load across the full streamflow range. While the exact reasons for this behavior require further investigation, possible explanations include that nitrate-N concentrations remained relatively constant across varying streamflows, leading to a linear response in daily nitrate-N load. Therefore, one linear equation is sufficient to represent the relationship between daily nitrate-N load and streamflow. In contrast, TN concentrations may increase sharply under high streamflow conditions due to the mobilization of organic N from stream banks and beds, resulting in a more complex phase response. These findings suggest that TN and nitrate-N exhibit different fate, transport, and loading mechanisms that have not been previously reported in the literature.

3.3. Seasonal N load

Sum of seasonal variations in TN and nitrate-N loads, along with streamflow, over the 31-year simulation period at the basin outlet were analyzed under both the base and afforestation scenarios (Fig. 5). Overall, sum of seasonal TN loads followed the order: spring (March–May) > winter (December–February) > summer (June–August) > fall (September–November) in both scenarios (Fig. 5a).Specifically, approximately half of the TN load occurred during spring - 50% in the afforestation scenario and 47% in the base scenario. A similar trend was observed for the sum of seasonal nitrate-N loads, which also followed the same descending order: spring > winter > summer > fall, with the highest loads consistently appearing in spring under both scenarios (Fig. 5b). This trend was largely attributed to seasonal variations in the sum of streamflow, as illustrated in Fig. 5c. The sum of streamflow exhibited the same seasonal pattern, peaking in spring, which directly influenced TN and nitrate-N transport and load in the watershed.

As discussed in the previous section, the higher the seasonal streamflow occurred, the larger the seasonal TN and nitrate-N loads happened. Additionally, springtime application of N fertilizers for crop cultivation significantly contributes to elevated N concentrations in stream water during this season. This seasonal spike aligns with findings from other studies. For example, Tian et al. (2020) projected the long-term N load from Mississippi River basin into the Gulf area and similarly reported that the highest N load occurred in spring, corroborating our simulation results. Analogous to the daily N load, significant differences in seasonal TN and nitrate-N loads between the base and afforestation scenarios were observed over the 31-year period (Table 2). As for the case of daily N load, afforestation fixes soil N through organic

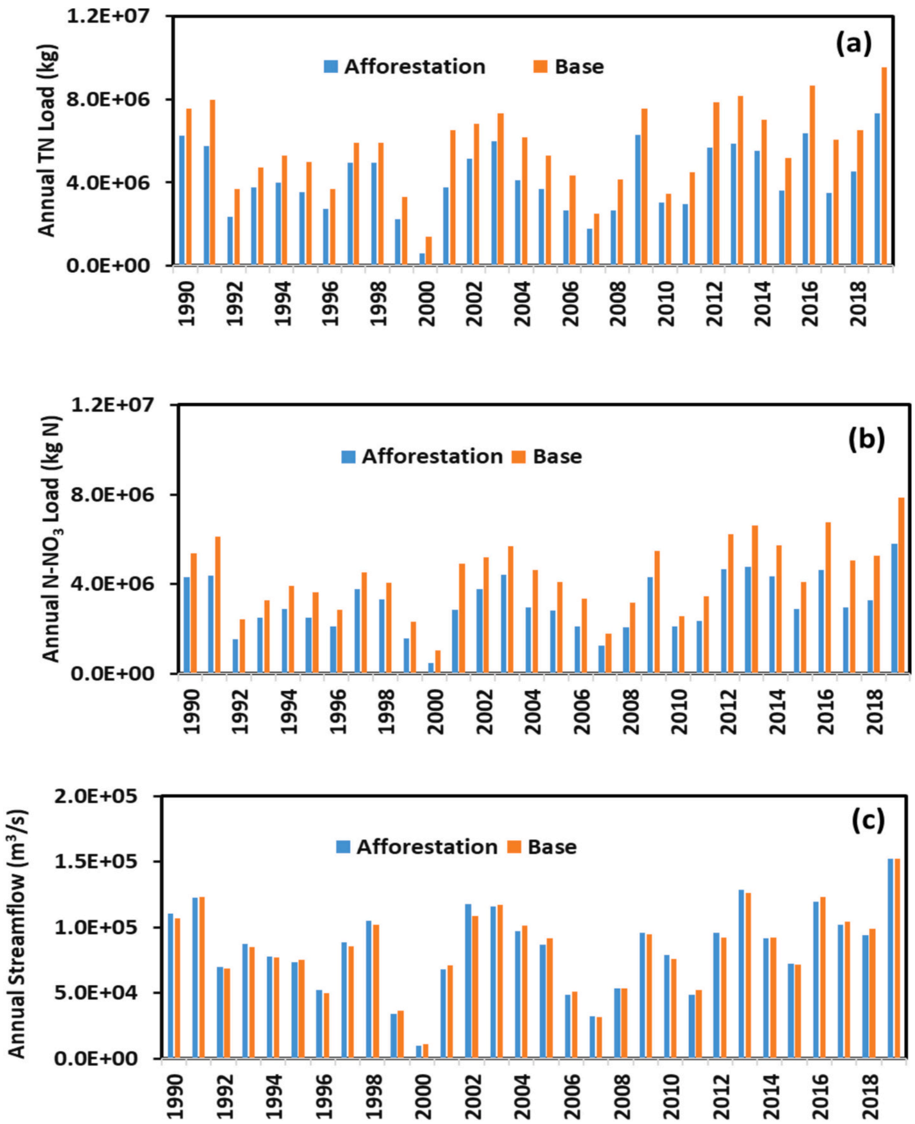

Fig. 6. Comparison of annual TN and nitrate-N loads and annual streamflow between the base and afforestation scenarios at the Pearl River basin outlet.

matter adsorption, decreases soil N content due to stronger tree root uptake, and reduces surface water runoff by intercepting rainwater and acting as a physical buffer. All these mechanisms alleviate N load to streams.

Interestingly, strong linear correlations were observed between sum of seasonal streamflow and sum of seasonal TN load in both the base and afforestation scenarios (Fig. 5d and e). Similarly robust correlations were also found between seasonal streamflow and nitrate-N load (figures not shown), reinforcing the role of streamflow variability in N transport and load. These linear relationships suggest that sum of seasonal TN loads can be effectively estimated using sum of streamflow data, assuming empirical relationships are established. However, it is important to note that the slopes and intercepts of these equations may differ across regions and watersheds, due to variations in land use, soil types, and climatic conditions. Therefore, it is essential to develop reliable, site-specific empirical equations based on high-quality observational or simulation data for applications.

3.4. Annual N load

Over the 31-year simulation period, annual TN and nitrate-N loads at the PRB outlet were consistently higher in the base scenario than in the afforestation scenario (Fig. 6). The differences between the two scenarios were found to be statistically significant based on the K—S test (Table 2), indicating a clear impact of afforestation on N load reduction. The average annual TN and nitrate-N loads were 4.4 x 10^6kg and 2.7 $\times$ 10^6 kg, respectively, in the afforestation scenario, compared to 5.9 x 10^6kg and 3.8 $\times$ 10^6 kg in the base scenario. This corresponded to about 26% higher TN load and about 28% higher nitrate-N load in the base scenario. These substantial differences demonstrate that afforestation contributed to a significant reduction in annual N load from the PRB to the NGOA. While the conversion of the corn and soybean lands to mixed forest lands for afforestation occupied only 1% of the PRB area. This conversion accounted for 43% reduction of the total crop lands in the PRB. This reduction dramatically decreased N fertilizer applications and thus reduced TN load into the NGOA.

However, no significant differences in annual streamflow were detected between the base and afforestation scenarios (Table 2), suggesting that the impacts of afforestation on annual streamflow in this study were largely unaffected. As discussed in Section 3.1, although all corn and soybean lands have been converted to forest mixed lands, this conversion only accounted for 1% of the PRB's total area. This small portion of the converted lands was likely insufficient to induce measurable changes in overall streamflow at the basin outlet. These findings implied that annual streamflow was not a major driving force to reduce TN and nitrate-N loads after afforestation. We therefore

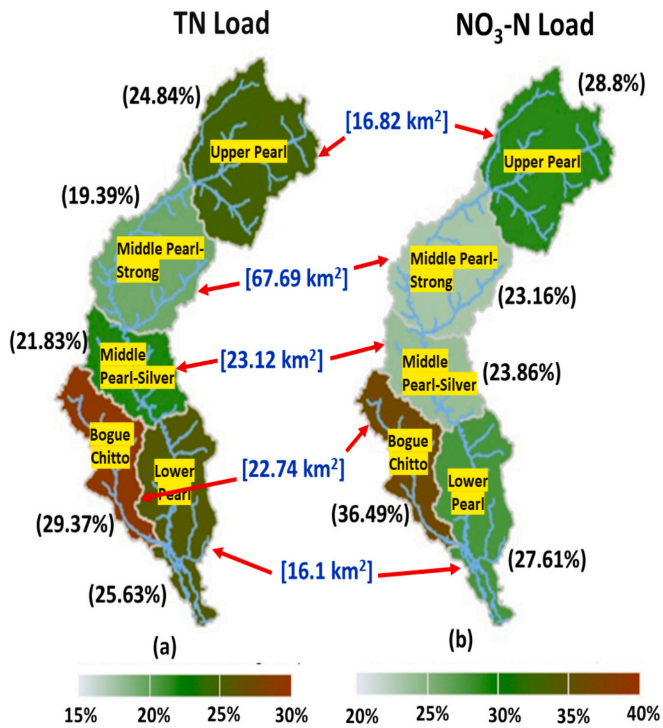

Fig. 7. Spatial distribution of percentage differences in TN and nitrate-N loads between the base and afforestation scenarios. The values in the parentheses are the average percentage differences, whereas the numbers in the brackets denote the areas used for converting corn and soybean lands to forest mixed lands.

attributed the reduction of TN and nitrate-N loads after afforestation to 1) the enhancement ofN adsorption and immobilization within forest soils, 2) reduced application of synthetic N fertilizers to afforested lands, and 3) decreased surface runoff and erosion, which are commonly observed following afforestation due to increased vegetative cover and improved soil structure(Meuser, 1990). In this study, the average surface runoff was about 51% higher in the base scenario than in the afforestation scenario although the percentage difference varied from watershed to watershed within the PRB. This finding confirmed that surface runoff play an important role in reducing N loading after afforestation. In this forest dominated basin (69%), the corn and soybean lands are primarily located at lowlands near riparian zones, and afforestation in these zones can effectively diffuse surface runoff and thereby reducing N load to the streams.

Fig. 6 further illustrates that annual TN and nitrate-N loads exhibited interannual variability in both scenarios (Fig. 6a and b), and these variations were positively correlated with fluctuations in annual streamflow (Fig. 6c). Years with higher streamflow volumes corresponded to increased N loads, highlighting the strong influence of streamflow on interannual N transport and loading. This reinforced the idea that, although overall streamflow volume did not differ significantly between the scenarios, year-to-year variability in streamflow still played a major role in shaping annual N loads.

The spatial distribution of the average percentage differences in annual TN and nitrate-N loads across the watersheds of the PRB is presented in Fig. 7. These values represent the difference between the base and afforestation scenarios, expressed as a percentage. Numbers in parentheses indicate the average percentage reduction, while numbers in brackets show the areas (in km^2) of corn and soybean lands converted to forest in each watershed. Notably, the extent of N load reduction was not directly proportional to the area of land converted. For example, in the Upper Pearl River watershed, a relatively small conversion area of 16.82 km^2 resulted in a 24.84% reduction in TN load, whereas the Middle Pearl-Strong River watershed saw a much larger conversion area of

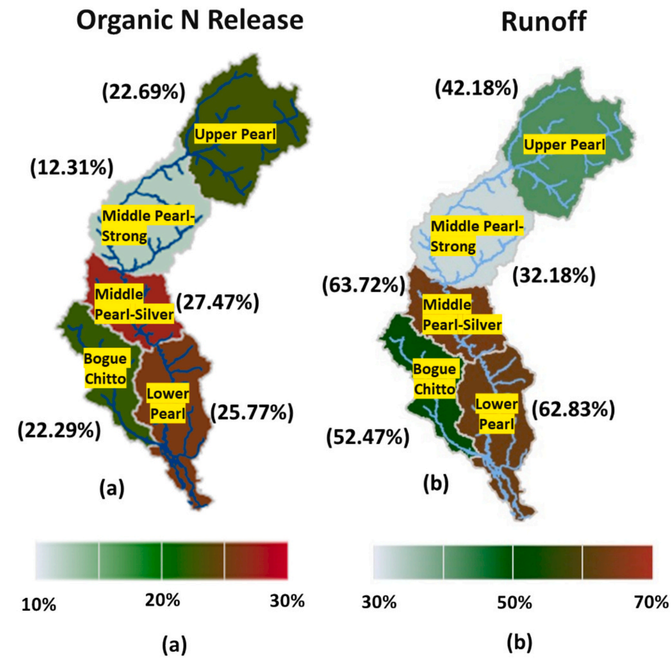

Fig. 8. Spatial distribution of percentage differences in organic N release and surface water runoff between the base and afforestation scenarios. The values in the parentheses are the average percentage differences.

67.69 km^2 but only achieved a 19.39% reduction (Fig. 7a). This disparity suggests that other spatial, chemical, physical, and ecological factors, including the specific location of afforestation (e.g., proximity to streams or riparian zones), land slope, soil properties, and the types of tree species planted, N adsorption, and surface water runoff, also significantly influence N load. Fig. 8 shows the percentage differences in annual average organic N release and surface water runoff between the base and afforestation scenarios among the five watersheds in the PRB over the 31-year simulation period. Overall, there was about 22% reduction in annual average organic N release in the PRB after afforestation and occurred partially due to soil N immobilization and partially due to other factors like surface water runoff reduction after afforestation. In this study, the average annual surface runoff reduced by about 51% in the PRB after afforestation (Fig. 8b). Zhai et al. (2023) found that afforestation with pure willow (*Salix babylonica*) and mulberry (*Morus alba*) in riparian zones of the upper Yangtze River, China led to substantial reductions in TN and nitrate-N concentrations in adjacent waterways. Such site-specific interventions enhance the interception and uptake of N before it reaches stream channels, effectively lowering N loads at the watershed scale. Results indicated that while afforestation in the PRB involved a relatively small land area, it still produced discernable and statistically significant reductions in N loads, primarily through improvements in land management and soil N dynamics rather than changes in streamflow. These findings highlight the importance of strategic site selection and ecologically informed design of afforestation efforts to optimize N load reduction in agricultural basins. Furthermore, the US-Environmental Protection Agency 2008 Gulf Hypoxia Action Plan established a 45 % TN load reduction goal to control the NGOA Hypoxia (https://www.epa.gov/ms-htf/gulf-hypoxia-action-plan-2008), and Xu et al. (2022) estimated that the opportunity cost to achieve that goal is about $6 billion annually. The result in this study has great implications in developing sound management strategies to reduce TN loading into NGOA with respect to tradeoffs between agricultural production and forestry

4. Conclusions

Comparisons of model predictions and field observations in streamflow and nitrogen (N) concentration during model calibrations and validations confirmed that the HAWQS model has good predictive performance in estimating TN and nitrate-N loads from the PRB into the NGOA.

Two distinct phases of daily TN load were found in both the base and afforestation scenarios: 1) the slow-loading phase at streamflow rates $\leq$1200 $m^3\ s^{-1}$ and 2) the rapid-loading phase at streamflow rates above 1200 $m^3\ s^{-1}$. This finding provides useful information to water resource managers on how to reduce daily N load through mitigating streamflow below a threshold value (i.e., 1200 $m^3\ s^{-1}$ for this study).

Average annual TN and nitrate-N loads were, respectively, 26% and 28% larger in the base scenario than in the afforestation scenario and were statistically significant based on the K—S test. These substantial differences demonstrated that afforestation contributed to a discernible reduction in annual N load into the NGOA. To date, little to no effort has been devoted to investigating the impacts of afforestation on N load into the NGOA, and this study has therefore filled this research gap.

Sum of seasonal TN and nitrate-N loads over the 31-year simulation period followed the order: spring > winter > summer > fall in both scenarios. About half of the loads occurred during spring in both the base and afforestation scenarios.

Reduction of TN and nitrate-N loads after afforestation could result from: 1) enhanced N adsorption and immobilization within forest soils, 2) reduced application of synthetic N fertilizers due to afforestation, and 3) decreased surface runoff and soil erosion. Furthermore, other factors, such as the specific location of afforestation (e.g., proximity to streams or riparian zones), land slope, soil properties, and the types of tree species planted, also significantly influence N load.

CRediT authorship contribution statement

Ying Ouyang: Writing – review & editing, Writing – original draft, Visualization, Validation, Software, Resources, Methodology, Formal analysis, Data curation, Conceptualization. **Johnny M. Grace:** Writing – review & editing. **Prem Parajuli:** Writing – review & editing. **Yongshan Wan:** Writing – review & editing, Investigation. **Yanbo Huang:** Writing – review & editing.

Declaration of competing interest

The authors declare that they have no known competing financial interests or personal relationships that could have appeared to influence the work reported in this paper.

Acknowledgement

The views expressed in this article are those of the authors and do not necessarily reflect the views or policies of the United State Department of Agriculture, the U.S. Environmental Protection Agency, and other agencies with which the authors are affiliated.

Data availability

Data will be made available on request.

References

Boz, B., Gumiero, B., 2016. Nitrogen removal in an afforested riparian zone: the contribution of denitrification processes. Hydrobiologia 774, 167–182.
Breitburg, D., Levin, L.A., Oschlies, A., Grégoire, M., Chavez, F.P., Conley, D.J., Garçon, V., Gilbert, D., Gutiérrez, D., Isensee, K., 2018. Declining oxygen in the global ocean and coastal waters. Science 359 (6371), eaam7240.
Chakravarty, S., Wang, Y., Zhou, M., 2021. Assessing Impacts of Deforestation on Water Quality in Agricultural Landscape in Indiana.
Chapman, E.L., Chambers, J.Q., Ribbeck, K.F., Baker, D.B., Tobler, M.A., Zeng, H.C., White, D.A., 2008. Hurricane Katrina impacts on forest trees of Louisiana's Pearl River basin. For. Ecol. Manag. 256 (5), 883–889.
Corona, J., Doley, T., Griffiths, C., Massey, M., Moore, C., Muela, S., Rashleigh, B., Wheeler, W., Whitlock, S.D., Hewitt, J., 2020. An integrated assessment model for valuing water quality changes in the United States. Land Econ. 96 (4), 478–492.
Dosskey, M.G., Bentrup, G., Schoeneberger, M., 2012. A role for agroforestry in Forest restoration in the lower Mississippi Alluvial Valley. J. Forest 110 (1), 48–55.
Fant, C., Srinivasan, R., Boehlert, B., Rennels, L., Chapra, S.C., Strzepek, K.M., Corona, J., Allen, A., Martinich, J., 2017. Climate change impacts on US water quality using two models: HAWQS and US basins. Water-Sui 9 (2), 118.
Goolsby, D.A., Battaglin, W.A., 2001. Long-term changes in concentrations and flux of nitrogen in the Mississippi River basin, USA. Hydrol. Process. 15 (7), 1209–1226.
Goolsby, D.A., Battaglin, W.A., Aulenbach, B.T., Hooper, R.P., 2001. Nitrogen input to the Gulf of Mexico. J. Environ. Qual. 30 (2), 329–336.
Haghverdi, K., Kooch, Y., 2020. Long-term afforestation effect and help to optimize degraded forest lands and reducing climate changes. Ecol. Eng. 142, 105656.
HAWQS_2.0, 2023. HAWQS System 2.0 and Data to Model the Lower 48 Conterminous U.S using the SWAT Model.
Jiang, K., Li, Z., Luo, C., Wu, M., Chao, L., Zhou, Q., Zhao, H., 2019. The reduction effects of riparian reforestation on runoff and nutrient export based on AnnAGNPS model in a small typical watershed, China. Environ. Sci. Pollut. R. 26, 5934–5943.
Li, M., Zhou, X., Zhang, Q., Cheng, X., 2014. Consequences of afforestation for soil nitrogen dynamics in Central China. Agric. Ecosyst. Environ. 183, 40–46.
Lu, C.Q., Zhang, J.E., Tian, H.Q., Crumpton, W.G., Helmers, M.J., Cai, W.J., Hopkinson, C.S., Lohrenz, S.E., 2020. Increased extreme precipitation challenges nitrogen load management to the Gulf of Mexico. Commun. Earth Environ. 1 (1).
MDEQ, 2007. Citizen's Guide to Water Quality in the Pearl River Basin.
Meuser, A., 1990. Effects of afforestation on run-off characteristics. Agric. For. Meteorol. 50 (1–2), 125–138.
Mitsch, W.J., Day, J.W., 2006. Restoration of wetlands in the Mississippi-Ohio-Missouri (MOM) river basin: experience and needed research. Ecol. Eng. 26 (1), 55–69.
Ouyang, Y., Leininger, T.D., Moran, M., 2015. Estimating effects of reforestation on nitrogen and phosphorus load reductions in the lower Yazoo River watershed, Mississippi. Ecol. Eng. 75, 449–456.
Ouyang, Y., Huang, Y.B., Parajuli, P.B., Wan, Y.S., Grace, J.M., Caldwell, P.V., Trettin, C., 2023. Projection of sediment loading from Pearl River Basin, Mississippi into Gulf of Mexico under a future climate with afforestation. Climate 11 (5).
Parajuli, P.B., 2010. Assessing sensitivity of hydrologic responses to climate change from forested watershed in Mississippi. Hydrol. Process. 24 (26), 3785–3797.
Qiu, Z., Shi, C., Zhao, M., Wang, K., Zhang, M., Wang, T., Shi, F., 2022. Improving effects of afforestation with different forest types on soil nutrients and bacterial community in Barren Hills of North China. Sustainability 14 (3), 1202.
Rabalais, N.N., Turner, R.E., 2019. Gulf of Mexico hypoxia: past, present, and future. Limnol. Oceanogr. Bull. 28 (4), 117–124.
Rabalais, N.N., Turner, R.E., Scavia, D., 2002a. Beyond science into policy: Gulf of Mexico hypoxia and the Mississippi River: nutrient policy development for the Mississippi River watershed reflects the accumulated scientific evidence that the increase in nitrogen loading is the primary factor in the worsening of hypoxia in the northern Gulf of Mexico. Bioscience 52 (2), 129–142.
Rabalais, N.N., Turner, R.E., Wiseman Jr., W.J., 2002b. Gulf of Mexico hypoxia, aka "The dead zone". Annu. Rev. Ecol. Syst. 33 (1), 235–263.
Rabalais, N.N., Turner, R.E., Sen Gupta, B.K., Platon, E., Parsons, M.L., 2007. Sediments tell the history of eutrophication and hypoxia in the northern Gulf of Mexico. Ecol. Appl. 17 (5), S129–S143.
Rasmussen, L., 1998. Effects of afforestation and deforestation on the deposition, cycling and leaching of elements. Agric. Ecosyst. Environ. 67 (2–3), 153–159.
Ryu, K., Watanabe, M., Shibata, H., Takagi, K., Nomura, M., Koike, T., 2009. Ecophysiological responses of the larch species in northern Japan to environmental changes as a basis for afforestation. Landsc. Ecol. Eng. 5, 99–106.
Shi, S.-w., Han, P.-f., Zhang, P., Ding, F., Ma, C.-l., 2015. The impact of afforestation on soil organic carbon sequestration on the Qinghai plateau, China. PLoS One 10 (2), e0116591.
Solari, M.E., 1967. Chakravarti,Im - Handbook of methods of applied statistics. Nature 216 (5118), 901.
Stanturf, J.A., Gardiner, E.S., Hamel, P.B., Devall, M.S., Leininger, T.D., Warren, M.E., 2000. Restoring bottomland hardwood ecosystems in the lower Mississippi Alluvial Valley. J. Forest 98 (8), 10–16.
Tian, H., Xu, R., Pan, S., Yao, Y., Bian, Z., Cai, W.J., Hopkinson, C.S., Justic, D., Lohrenz, S., Lu, C., 2020. Long-term trajectory of nitrogen loading and delivery from Mississippi River basin to the Gulf of Mexico. Global Biogeochem. Cy. 34 (5), e2019GB006475.
Turner, R.E., Rabalais, N.N., 2022. Forecast: Summer Hypoxic Zone Size Northern Gulf of Mexico. https://gulfhypoxia.net/wp-content/uploads/2022/06/2022-hypoxia-forecast_NR.pdf (accessed on November, 7, 2025).
Xu, Y., Elbakidze, L., Yen, H., Arnold, J.G., Gassman, P.W., Hubbart, J., Strager, M.P., 2022. Integrated assessment of nitrogen runoff to the Gulf of Mexico. Resour. Energy Econ. 67, 101279.
Yen, H., Daggupati, P., White, M.J., Srinivasan, R., Gossel, A., Wells, D., Arnold, J.G., 2016. Application of large-scale, multi-resolution watershed modeling framework using the hydrologic and water quality system (HAWQS). Water-Sui 8 (4).